

Enhanced optomechanical entanglement and cooling via dissipation engineering

Yan-Lei Zhang,^{1,2} Chuan-Sheng Yang,^{1,2} Zhen Shen,^{1,2} Chun-Hua Dong,^{1,2} Guang-Can Guo,^{1,2} Chang-Ling Zou,^{1,2,*} and Xu-Bo Zou^{1,2,†}

¹CAS Key Laboratory of Quantum Information, University of Science and Technology of China, Hefei, Anhui 230026, China

²CAS Center For Excellence in Quantum Information and Quantum Physics, University of Science and Technology of China, Hefei, Anhui 230026, China

(Dated: February 2, 2022)

We propose an optomechanical dissipation engineering scheme by introducing an ancillary mechanical mode with a large decay rate to control the density of states of the optical mode. The effective linewidth of the optical mode can be reduced or broadened, manifesting the dissipation engineering. To prove the ability of our scheme in improving the performances of the optomechanical system, we studied optomechanical entanglement and phonon cooling. It is demonstrated that the optomechanical entanglement overwhelmed by thermal phonon excitations could be restored via dissipation engineering. For the phonon cooling, an order of magnitude improvement could be achieved. Our scheme can be generalized to other systems with multiple bosonic modes, which is experimentally feasible with advances in materials and nanofabrication, including optical Fabry-Perot cavities, superconducting circuits, and nanobeam photonic crystals.

I. INTRODUCTION

In recent years, optomechanical systems [1–4] have attracted considerable attention in classical and quantum information processing. Dramatic theoretical and experimental progress has been achieved in the optomechanically induced transparency [5, 6], sensing [4], frequency combs [7], and tunable optical filters [8]. For potential applications in the quantum regime [1, 9–11], ground-state cooling of the mechanical resonator [12, 13], optomechanical entanglement and squeezing [14–16], and quantum sensors [17, 18] have been studied. Most researches have focused on canonical systems with only one optical and mechanical degree of freedom. For multimode optomechanical systems [19–22], more degrees of freedom can be controlled, and new phenomena are observed and new functionalities are realized, such as optomechanical induced nonreciprocity [23], circulators [24, 25], and coherent frequency convertor [26, 27]. However, the interplay between different optomechanical interactions and different mechanical or optical modes are omitted in previous studies.

On the other hand, dissipation engineering [28–31] has been developed in quantum optics. By introducing dissipative modes into the quantum system, the density of states of the system can be efficiently controlled and thus suppresses unwanted physical processes or induces desired interactions. Recently, dissipation engineering has been widely used to generate steady entanglement in superconducting qubits [32, 33], trapped ions [34, 35], superconducting resonators [36], and Rydberg atoms [37]. Therefore, it is expected to introduce this beneficial idea to the optomechanical system. In practical, most optomechanical systems naturally support the multimodes [4, 38–40], and these modes can be excited by polychromatic laser drive [41]. With the advantages of multiple degrees in multimode optomechanical systems [42], dissipation engineering [43] holds huge potential in all-optical information processing [32, 44, 45], where two or more mechanical or optical modes lead to a wealth of different possible schemes.

In this paper, we theoretically analyze a multimode optomechanical system, where Brillouin phonon mode and breath mechanical mode are coupled with a common optical mode. The Brillouin phonon mode serves as an ancillary, which is used to engineer the optical density of state and thus realize the dissipation engineering. The effect of dissipation engineering is studied in different aspects, including optomechanical induced transparency (OMIT) and optomechanical induced amplification (OMIA), entanglement between the optical mode and breath mechanical mode, and cooling of the breath mechanical mode. The enhancement of the entanglement or cooling is obtained for certain dissipation engineering strength, and the numerical results reveal the potential of our scheme. On the other hand, the extra noises introduced by the ancillary mode and strong modification of the optical mode could also suppress the performance of an optomechanical system, suggesting an optimal dissipation engineering that balances the positive and negative effects. Our scheme could be generalized to other nonlinear interactions in multiple mode systems, such as atom ensemble and Fabry-Perot (FP) cavity system [46] and superconducting circuits [47], and finds applications in quantum devices [48].

II. THE SYSTEM

We consider a multimode optomechanical system [25, 49, 50], and its schematic is shown in Fig. 1(a), where two mechanical modes (b , m) are coupled with a common optical mode a . The interaction Hamiltonian can be described by ($\hbar = 1$):

$$H_{\text{int}} = G_b b (a^\dagger + a) + G_m a (m^\dagger + m) + \text{H.c.}, \quad (1)$$

where $G_{b(m)}$ is the pump laser stimulated effective coupling between the modes. Here, we focus on the modes a , m , and the mode b is treated as an ancillary mode, which is encircled with a dashed line. By the interaction G_b , we can modulate the mode a , which further affects the effective coupling between

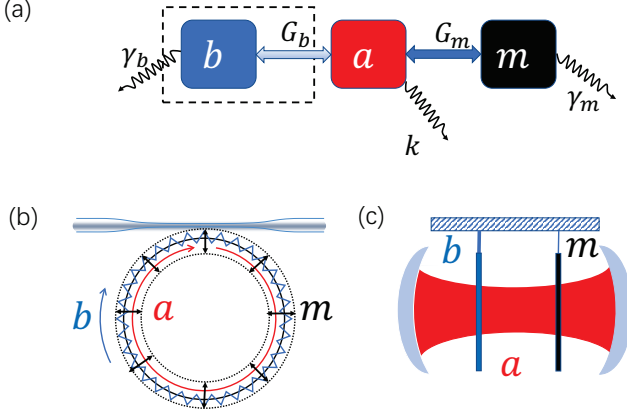


FIG. 1. (Color online) (a) Schematic of the multimode optomechanical system for dissipation engineering. Potential experimental systems: (b) the optical microresonator, where both the Brillouin mechanical mode b and the breath mechanical mode m are coupling to the common optical mode a ; (c) the Fabry-Perot cavity with two mechanical membranes inside, the optical mode a can simultaneously couple with mechanical modes b and m in different membranes.

the modes a and m . The dissipation engineering scheme can be realized in many physical systems, in which two potential systems are the optical microresonator [25] and FP cavity [51], as shown in Figs. 1(b) and (c), respectively. In the FP cavity, the scheme can be easily realized with two driving lasers, and two mechanical modes b , m are coupled with the optical mode a by the red or blue detuned pump lasers. The scheme can be also generalized to other bosonic systems, including magnon [52], atomic spin excitation [53], and photonic crystals [54].

In the following, we focus on an experimentally optomechanical system based on the on-chip optical microresonator, where the coherent couplings between the optical mode and the Brillouin phonon mode ($\sim 10\text{GHz}$) [55], breath mechanical mode ($\sim 100\text{MHz}$) [23] can be stimulated simultaneously by external laser pumps. The full system can be described by the following Hamiltonian

$$H_{\text{sys}} = H_0 + H_{\text{SBS}} + H_{\text{BM}} + H_{\text{D}}, \quad (2)$$

where

$$H_0 = \omega_j a_j^\dagger a_j + \omega_k a_k^\dagger a_k + \omega_b b_{j-k}^\dagger b_{j-k} + \omega_m m^\dagger m, \quad (3)$$

$$H_{\text{SBS}} = g_b (a_j^\dagger a_k b_{j-k} + a_j a_k^\dagger b_{j-k}^\dagger), \quad (4)$$

$$H_{\text{BM}} = g_{m,j} a_j^\dagger a_j (m + m^\dagger) + g_{m,k} a_k^\dagger a_k (m + m^\dagger), \quad (5)$$

$$H_{\text{D}} = i\sqrt{\kappa_{j,\text{ex}}}\epsilon_{d,j} \left(a_j^\dagger e^{-i\omega_{d,j}t} - a_j e^{i\omega_{d,j}t} \right) + i\sqrt{\kappa_{k,\text{ex}}}\epsilon_{d,k} \left(a_k^\dagger e^{-i\omega_{d,k}t} - a_k e^{i\omega_{d,k}t} \right). \quad (6)$$

Here H_0 describes four eigenmodes of the system, including two optical modes (a_j , a_k) and two mechanical modes (b_{j-k} , m); H_{SBS} describes the triple-resonant stimulated Brillouin scattering between the high-frequency traveling phonon

mode and two optical modes, and H_{BM} is the dispersive optomechanical coupling between the breath mechanical mode and optical mode; H_{D} represents the external laser driving onto the optical modes. $a_{j(k)}$ is the annihilation operator for optical mode $j(k)$ with the frequency $\omega_{j(k)}$, b_{j-k} is the annihilation operator of the Brillouin mechanical mode with the frequency ω_b , m is the annihilation operator of the breath mechanical mode with the frequency ω_m , g_b is the triple-resonant coupling strength of the stimulated Brillouin scattering, $g_{m,j(k)}$ is the dispersive coupling rate, $\epsilon_{d,j(k)}$ is the driving field of the optical mode $a_{j(k)}$ with a frequency $\omega_{d,j(k)}$, and $\kappa_{j(k),\text{ex}}$ is the external coupling rate. For the stimulated Brillouin scattering, we need both the energy and momentum conservation, so $\omega_j = \omega_k + \omega_b$ is also satisfied.

For a very weak coupling rate g_0 , g_j , $g_k \ll \omega_b$, ω_m , $\kappa_{j(k)}$, where $\kappa_{j(k)} = \kappa_{j(k),o} + \kappa_{j(k),\text{ex}}$ is the total optical energy decay rate, the optomechanical interactions can be enhanced by the control laser $\epsilon_{d,j(k)}$. When the duration of the control pulse $\tau_d \gg 1/\kappa_{j(k)}$, the intracavity control fields can be treated classically as:

$$\alpha_{j(k)} = \frac{\sqrt{\kappa_{j(k),\text{ex}}}\epsilon_{d,j(k)}}{\kappa_{j(k)}/2 + i\Delta_{j(k)}}, \quad (7)$$

where $\Delta_{j(k)} = \omega_{j(k)} - \omega_{d,j(k)}$. In the interaction picture $H_0 = \omega_{d,j} a_j^\dagger a_j + \omega_{d,k} a_k^\dagger a_k + (\omega_{d,j} - \omega_{d,k}) b_{j-k}^\dagger b_{j-k}$, the Hamiltonian of the system can be linearized as

$$H_{\text{lin}} \approx \Delta_j a_j^\dagger a_j + \Delta_k a_k^\dagger a_k + \Delta_b b_{j-k}^\dagger b_{j-k} + \omega_m m^\dagger m + G_{b,j} a_k^\dagger b_{j-k}^\dagger + G_{b,k} a_j^\dagger b_{j-k} + \text{H.c.} + \left(G_{m,j} a_j^\dagger + G_{m,k} a_k^\dagger + \text{H.c.} \right) (m^\dagger + m), \quad (8)$$

where $\Delta_b = \omega_b + \omega_{d,k} - \omega_{d,j}$, $G_{b,j(k)} = g_b \alpha_{j(k)}$, and $G_{m,j(k)} = g_{m,j(k)} \alpha_{j(k)}$.

III. DISSIPATION ENGINEERING

Firstly, we only consider the stimulated Brillouin scattering, as the mechanical mode b_{j-k} is used as an ancillary to engineer the optical mode. For the stimulated Brillouin scattering, the triple-resonant condition is required [41, 55]. For simplification, we assume that one driving laser is on-resonant with the optical mode, i.e. $\Delta_j = 0$ or $\Delta_k = 0$. By treating the laser pump on a_j as a classical field, we can write the effective Hamiltonian as $H_{\text{SBS}} = G_{b,j} a_k^\dagger b_{j-k}^\dagger + G_{b,j}^* a_k b_{j-k}$. Such a stimulated Brillouin scattering is a Stokes process, which generates photon-phonon pairs into the system, thus eventually induces gain to the system and reduces the linewidth of the optical mode a_k .

To observe the effect of dissipation engineering on the optical linewidth, a weak probe laser is sent into the optical mode

a_k , and the Langevin equations can be written as follows

$$\frac{d}{dt}a_k = -\left(\frac{\kappa_k}{2} - i\delta\right)a_k - iG_{b,j}b_{j-k}^\dagger + \sqrt{\kappa_{k,ex}}\varepsilon_{p,k}, \quad (9)$$

$$\frac{d}{dt}b_{j-k}^\dagger = -\left(\frac{\gamma_b}{2} - i\delta\right)b_{j-k}^\dagger + iG_{b,j}^*a_k, \quad (10)$$

where $\delta = \omega_p - \omega_k$, γ_b is the Brillouin mechanical decay rate, and $\varepsilon_{p,k}$ is the probe laser with the frequency ω_p . When the system is at the steady state, which requires that the optomechanical coupling is below the lasing threshold [56], we have $a_k(\delta) = \sqrt{\kappa_{k,ex}}\varepsilon_{p,k}/(\kappa_{\text{eff}}/2 - i\delta)$, where the effective dissipation rate and detuning of the optical mode can be written as

$$\kappa_{\text{eff}} = \kappa_k - \frac{|G_{b,j}|^2\gamma_b}{\left(\frac{\gamma_b}{2}\right)^2 + \delta^2}, \quad (11)$$

$$\delta_{\text{eff}} = \delta + \frac{|G_{b,j}|^2\delta}{\left(\frac{\gamma_b}{2}\right)^2 + \delta^2}. \quad (12)$$

If these parameters satisfy δ , $|G_{b,j}|$, $\kappa_k \ll \gamma_b$, we can obtain the effective decay rate $\kappa_{\text{eff}} \approx \kappa_k - 4|G_{b,j}|^2/\gamma_b$ and the effective detuning $\delta_{\text{eff}} \approx \delta$.

If we consider the driving laser resonant with the optical mode a_k , the stimulated Brillouin scattering is an anti-Stokes process, and the effective Hamiltonian can be written as $H_{\text{SBS}} = G_{b,k}a_j^\dagger b_{j-k} + G_{b,k}^*a_j b_{j-k}^\dagger$. As opposed to the Stokes process, the particle number conserves and the coupling would introduce extra loss channel to the optical mode. Similarly, then the effective decay rate is derived as $\kappa_{\text{eff}} \approx \kappa_j + 4|G_{b,k}|^2/\gamma_b$, which confirms that linewidth of the optical mode a_j is broadened due to b . In practical experiments, we can detect the intracavity power to show the variation of the optical mode linewidth. For the sake of illustration, we can normalize the intracavity power as

$$P_a(\delta) = \left| \frac{\kappa_{\text{eff}}}{2\sqrt{\kappa_{k,ex}}\varepsilon_p} a \right|^2, \quad (13)$$

where we have omitted the subscript of some parameters for convenience.

In Fig. 2(a), we plot the intracavity power P_a as a function of the detuning δ . The blue and red lines correspond to the case that the control laser is added into the optical mode a_j and a_k , respectively, and the black line is the result without the control laser ($G_b = 0$) for comparison. The dashed and dotted lines are corresponding to the effective coupling $G_b/(2\pi) = 2$ and 3 MHz, respectively. When $\Delta_j = 0$, the blue lines show that the effective linewidth of the optical mode is reduced with the increasing of the control powers, and the intracavity power spectra agree with the theoretical result $\kappa_{\text{eff}} = \kappa_k - 4|G_{b,j}|^2/\gamma_b$. For $\Delta_k = 0$, the related results are plotted by the red lines, which show that the broadened linewidth of the optical mode as $\kappa_{\text{eff}} = \kappa_j + 4|G_{b,k}|^2/\gamma_b$. Based on the analytical derivations and numerical calculation above, we conclude that the effective linewidth of the optical mode can be effectively reduced or broadened by the dissipation engineering.

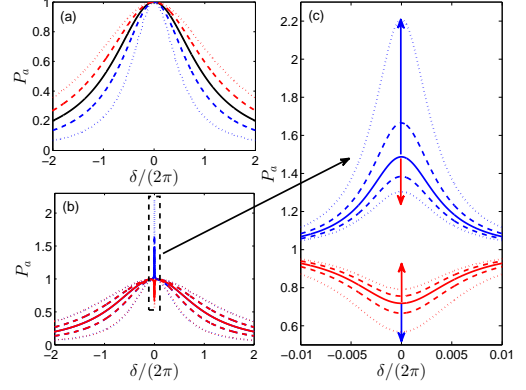


FIG. 2. (Color online) Intracavity power P_a of the optical mode a . (a) Engineering the linewidth of the optical mode via only stimulated Brillouin scattering. The intracavity power spectra for different control powers $G_b/(2\pi) = 0$ (solid line), 2 (dashed line), and 3 (dotted line) MHz, where the blue and red lines are corresponding to $\Delta_j = 0$ and $\Delta_k = 0$, respectively. (b) Optomechanical induced transparency and amplification are affected by the dissipation engineering, and (c) is the enlarged view of the (b) around the detuning $\delta/(2\pi) \in [-0.01, 0.01]$ MHz. The intracavity power spectra for the red detuning $\Delta_{j(k)} = \omega_m$ and the blue detuning $\Delta_{j(k)} = -\omega_m$ with the control power $G_{m,j(k)}/2\pi = 0.03$ MHz, where the blue and red arrows are corresponding to $\Delta_j = 0$ (Stokes process) and $\Delta_k = 0$ (anti-Stokes process), respectively. Other parameters are $\kappa_j/2\pi = 2$ MHz, $\kappa_k/2\pi = 2$ MHz, $\gamma_b/2\pi = 40$ MHz, $\omega_b/2\pi = 10$ GHz, $\gamma_m/2\pi = 10$ kHz and $\omega_m/2\pi = 100$ MHz.

Now we consider the breath mechanical mode m for the radiation pressure optomechanical coupling, where the OMIT or OMIA can be observed due to another drive laser that induces coherent photon-phonon interaction. From Fig. 2(a), we know that the effective linewidth of the optical mode can be modulated by the stimulated Brillouin scattering, which indicates that the OMIT and OMIA can be effectively controlled by the dissipation engineering. For the radiation pressure optomechanical coupling, the drive can be either red or blue detuning $\Delta_{j(k)} = \pm\omega_m$. Combining the stimulated Brillouin scattering and optomechanical couplings, we can divide possible experimental configurations into four cases: (a) anti-Stokes process and red detuning: $\Delta_k = 0$, $\Delta_j = \omega_m$; (b) anti-Stokes process and blue detuning: $\Delta_k = 0$, $\Delta_j = -\omega_m$; (c) Stokes process and red detuning: $\Delta_j = 0$, $\Delta_k = \omega_m$; (d) Stokes process and blue detuning: $\Delta_j = 0$, $\Delta_k = -\omega_m$. To illustrate different situations intuitively, we add a weak laser to probe the optical mode a . Firstly, we consider the case (a) and the corresponding Hamiltonian of the system can be written as

$$H = -\delta a^\dagger a - \delta b^\dagger b - \delta m^\dagger m + (G_b a^\dagger b + G_m a^\dagger m + \text{H.C.}) + i\sqrt{\kappa_{k,ex}}\varepsilon_p (a^\dagger - a), \quad (14)$$

where $\delta = \omega_p - \omega_j$. We have omitted the subscript of some parameters for convenience and neglected other terms with the rotating wave approximation $\omega_m \gg \kappa_{j(k)}, \gamma_m$, where γ_m is the

breath mechanical decay rate. The steady state solution reads

$$a(\delta) = \frac{\sqrt{\kappa_{ex}} \varepsilon_p}{\frac{\kappa}{2} - i\delta + \frac{G_b^2}{\gamma_b/2 - i\delta} + \frac{G_m^2}{\gamma_m/2 - i\delta}}. \quad (15)$$

For the convenience, we have assumed that G_b and G_m are real numbers. When we consider other cases (b,c,d), the steady state solution has a similar form to the above equation and we only change the couplings: $G_b^2 \rightarrow -G_b^2$ for the Stokes process; $G_m^2 \rightarrow -G_m^2$ for the blue detuning.

In Figs. 2(b) and (c), we discuss the dissipation engineering on both the OMIT and OMIA, and we plot the normalized intracavity power P_a as the function of the detuning between the probe laser and the optical cavity. When the probe drive is largely detuned from the mechanical resonance, the effect due to radiation pressure optomechanical coupling is almost not observable, where the Fig. 2(b) is almost the same as Fig. 2(a). Figure 2(c) is the magnification of Fig. 2(b) around the detuning $\delta/(2\pi) \in [-0.01, 0.01]$ MHz. The arrows mean that the OMIT and OMIA is enhanced (the blue arrow) or suppressed (the red arrow) with the increasing of dissipation engineering (G_b). Here the parameters that we choose satisfy $\gamma_b \gg \kappa_{k(j)}, \gamma_m$, and we only consider the detuning $|\delta| \ll \gamma_b$. These phenomena can be described by the approximate emission power spectra

$$P_a \approx \left| \frac{1}{1 - 2i\delta/\kappa_{\text{eff}} \pm \frac{C}{1 - 2i\delta/\gamma_m}} \right|^2, \quad (16)$$

where the cooperativity $C = 4|G_m|^2/(\kappa_{\text{eff}}\gamma_m)$ and \pm for the blue and red detuning. For a fixed G_m , it is obvious that the OMIT and OMIA are controlled by the effective linewidth of the optical mode $\kappa_{\text{eff}} = \kappa \pm 4|G_b|^2/\gamma_b$.

From Fig. 2, it is demonstrated that the dissipation engineering could modulate the linewidth of optical mode, which can be used to control the OMIT and OMIA. Especially, it can also make the unresolvable sideband in the optomechanical system, i.e. $\omega_m < \kappa_{\text{eff}}$, to be resolvable by reducing the linewidth of the optical mode.

IV. ENTANGLEMENT AND COOLING

Next, we discuss the effect of the dissipation engineering on the entanglement of radiation pressure optomechanical system and cooling of the mechanical mode m . It is known that the thermal noise is bad for the entanglement [50] and cooling, so we only consider the anti-Stokes process as the dissipation engineering to cool the system. For the stimulated Brillouin scattering, we consider the driving laser is resonant with the optical mode a_k . The Hamiltonian of the system can be written as

$$H = \Delta_j a_j^\dagger a_j + \Delta_b b_{j-k}^\dagger b_{j-k} + \omega_m m^\dagger m + \left[G_{b,k} a_j^\dagger b_{j-k} + G_{m,j} a_j^\dagger (m^\dagger + m) + \text{H.C.} \right]. \quad (17)$$

We define $R = (q_a, p_a, q_b, p_b, q_m, p_m)^T$, where $q_o = (o^\dagger + o)/\sqrt{2}$ and $p_o = i(o^\dagger - o)/\sqrt{2}$. The Langevin equations can be written as

$$\frac{d}{dt}R = MR + R_{\text{in}}, \quad (18)$$

where

$$M = \begin{bmatrix} -\frac{\kappa_k}{2} & \Delta_j & 0 & G_{b,k} & 0 & 0 \\ -\Delta_j & -\frac{\kappa_k}{2} & -G_{b,k} & 0 & -2G_{m,j} & 0 \\ 0 & G_{b,k} & -\frac{\gamma_b}{2} & \Delta_b & 0 & 0 \\ -G_{b,k} & 0 & -\Delta_b & -\frac{\gamma_b}{2} & 0 & 0 \\ 0 & 0 & 0 & 0 & -\frac{\gamma_m}{2} & \omega_m \\ -2G_{m,j} & 0 & 0 & 0 & -\omega_m & -\frac{\gamma_m}{2} \end{bmatrix}, \quad (19)$$

and the thermal noise can be written as $R_{\text{in}} = (\sqrt{\kappa_j} q_a^{\text{in}}, \sqrt{\kappa_j} p_a^{\text{in}}, \sqrt{\gamma_b} q_b^{\text{in}}, \sqrt{\gamma_b} p_b^{\text{in}}, \sqrt{\gamma_m} q_m^{\text{in}}, \sqrt{\gamma_m} p_m^{\text{in}})^T$. Here we have assumed that the $G_{b,k}$ and $G_{m,j}$ are the real numbers. The fact that the dynamics of the system is governed by a linearized Hamiltonian ensures that the evolved states are Gaussian states whose information-related properties [57] are fully represented by the 6×6 covariance matrix with entries defined as

$$V_{i,j} = \langle R_i R_j + R_j R_i \rangle / 2. \quad (20)$$

The equation of motion corresponding to the covariance matrix can be written as follows

$$\frac{d}{dt}V = MV + VM^T + D, \quad (21)$$

where $D = \text{Diag} \left(\frac{\kappa_k}{2}, \frac{\kappa_k}{2}, \frac{\gamma_b}{2}, \frac{\gamma_b}{2}, \frac{\gamma_m(2n_m+1)}{2}, \frac{\gamma_m(2n_m+1)}{2} \right)$. For $\omega_b \gg \omega_m$, we have neglected the thermal noise of the mode b .

A. Entanglement

The entanglement between optical mode and mechanical mode is generated by the interaction term $G_{m,j} a_j^\dagger m^\dagger + \text{H.c.}$, so we choose the detuning $\Delta_j = \Delta_b = -\omega_m$. The continuous variable entanglement of two modes can be calculated by the logarithmic negativity E_N [58]. This quantity is a rigorous entanglement monotone, and is zero for separable states. For the two-mode Gaussian states, it can be calculated using the expression [49]

$$E_N = \max[0, -\ln(2\eta)], \quad (22)$$

where

$$\eta = \frac{1}{\sqrt{2}} \sqrt{\Sigma - \sqrt{\Sigma^2 - 4 \det V}}, \quad (23)$$

and $\Sigma = \det V_1 + \det V_2 - \det V_3$. The matrix V_1 , V_2 and V_3 are 2×2 matrices related to the covariance matrix as

$$V = \begin{bmatrix} V_1 & V_3 \\ V_3^T & V_2 \end{bmatrix}. \quad (24)$$

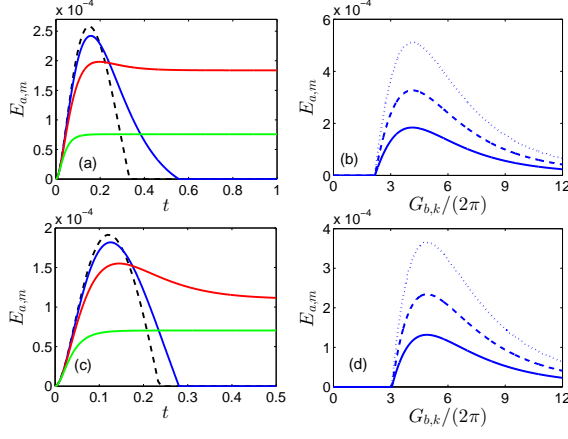


FIG. 3. (Color online) Logarithmic negativity E_{am} affected by the dissipation engineering. (a) The logarithmic negativity as a function of the time t with $G_{m,j}/(2\pi) = 0.03$ MHz for $G_{b,k}/(2\pi) = 0$ (black dashed line), 2 (blue line), 4 (red line), and 8 (green line) MHz. (b) The logarithmic negativity versus the dissipation engineering $G_{b,k}$ for $G_{m,j}/(2\pi) = 0.03$ (solid line), 0.04 (dashed line), 0.05 (dotted line) MHz. (a) and (b) are the results with the thermal noise $n_m = 250$; (c) and (d) are the condition with $n_m = 300$. Other parameters are the same as Fig. 2.

Here we only concern the entanglement of radiation pressure optomechanical system, so the covariance matrix V is about the modes a, m . In Fig. 3, we study the effect of dissipation engineering on the entanglement. The dynamical logarithmic negativity E_{am} with dissipation engineering is shown in Fig. 3(a). The black dashed line is the result without the dissipation engineering, and the E_{am} reaches a maximum at an appropriate evolution time. When the system approaches the steady-state, the entanglement disappears with $E_{am} = 0$ for the thermal noise n_m . The solid lines show the dissipation engineering on the entanglement, where $G_{b,k}/(2\pi) = 2$ (blue line) and 4 (red line) MHz, which mean that the steady logarithmic negativity E_{am} becomes bigger with the increasing of the dissipation engineering $G_{b,k}$. However, for stronger dissipation engineering $G_{b,k}/(2\pi) = 8$ (green line) MHz, it will reduce the steady logarithmic negativity, which means that there is the optimal engineering for the logarithmic negativity.

In Fig. 3(b), we plot the optimal engineering for different couplings $G_{m,j}/(2\pi) = 0.03$ (solid line), 0.04 (dashed line), 0.05 (dotted line) MHz, and the steady logarithmic negativity E_{am} has a peak. Because of the thermal noise n_m , there is a phase transition point for the entanglement growing out of nothing. For more thermal noise $n_m = 300$, the Figs. 3(c) and (d) show that the logarithmic negativity E_{am} becomes smaller and it needs more dissipation engineering to recover the entanglement.

For dissipation engineering, we also consider the effect of the detuning Δ_b on the stationary intracavity entanglement, which is shown in Fig. 4(a). Near the resonance point $\Delta_b = -\omega_m$, we obtain the maximal E_{am} , which is due to the most effective coupling at the resonance point. With the increase of the

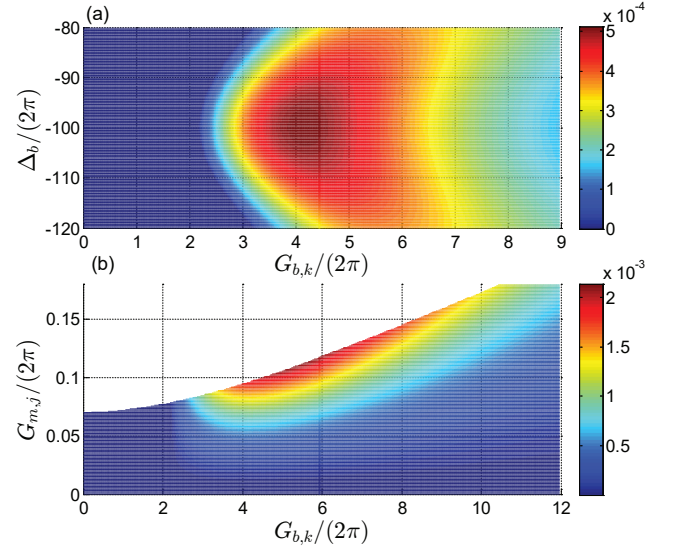


FIG. 4. (Color online) (a) Logarithmic negativity E_{am} as a function of both Δ_b and $G_{b,k}$ with $G_{m,j}/(2\pi) = 0.05$ MHz. (b) Logarithmic negativity E_{am} for both $G_{m,j}$ and $G_{b,k}$ with $\Delta_b = -\omega_m$. Here we choose the $n_m = 250$. Other parameters are the same as Fig. 2.

coupling $G_{m,j}$, we can always find an optimal $G_{b,k}$ for the stationary intracavity entanglement, as shown in Fig. 4(b). However, for the large $G_{m,j}$, the eigenvalues of M have a positive real part, which makes the system unstable. We can predicate stability conditions by the well-known Routh-Hurwitz criteria [59], which is labeled by the blank in Fig. 4(b). The maximal E_{am} is obtained at the edge of the unstable region, and the stable entanglement becomes weaker for the larger $G_{m,j}$.

From Figs. 3 and 4, we conclude that the noise-overwhelmed steady entanglement between the optical mode and mechanical mode can be restored by the dissipation engineering, which is robust to the thermal noise of the mechanical mode. It is due to the anti-Stokes process from the stimulated Brillouin scattering to cool the optomechanical system. For the strong dissipation engineering, the entanglement abates for the strong-nonlinearity.

B. Cooling

The dissipation engineering can be also used to enhance the cooling of the mechanical mode m . From the covariance matrix, the final steady thermal occupation of the mode m is calculated by

$$\langle m^\dagger m \rangle = n_f = \frac{V_{5,5} + V_{6,6} - 1}{2}. \quad (25)$$

The cooling is from the interaction term $G_{m,j}a_j^\dagger m + \text{H.c.}$ [4], so we choose the detuning $\Delta_j = \Delta_b = \omega_m$. In Fig. 5, we discuss the cooling effect of dissipation engineering. We plot the thermal occupation n_f as a function of $G_{m,j}$ in Fig. 5(a). The black dashed line is the result without the dissipation engineering,

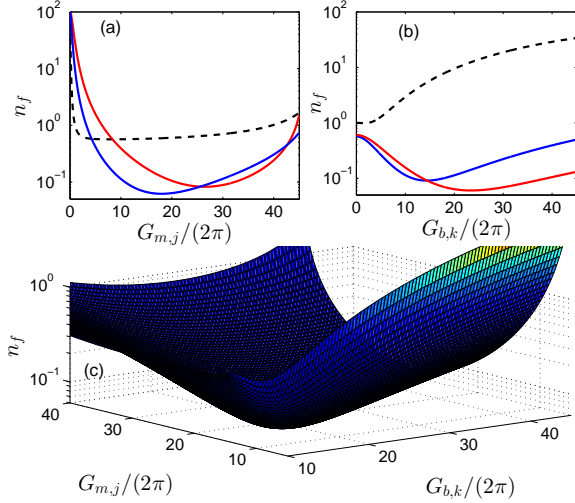


FIG. 5. (Color online) (a) The thermal occupation as a function of $G_{m,j}$ for $G_{b,k}/(2\pi) = 0$ (black dashed line), 20 (blue line) and 40 (red line) MHz. (b) The thermal occupation as a function of $G_{b,k}$ for $G_{m,j}/(2\pi) = 1$ (black dashed line), 10 (blue line) and 20 (red line) MHz. (c) Cooling effect for both $G_{m,j}$ and $G_{b,k}$. Here we choose the $n_m = 100$. Other parameters are the same as Fig. 2.

and the thermal noise reduces quickly with the increasing of $G_{m,j}$. And then it goes up slowly, which is corresponding to the term $G_{m,j}a_j^\dagger m^\dagger + \text{H.c.}$, where the rotating wave approximation is not well satisfied for very large $G_{m,j}$. When $G_{b,k}/(2\pi) = 20$ MHz, we plot the blue line, and the cooling effect becomes worse than no dissipation engineering in the weak coupling area, where $G_{m,j}/(2\pi) \leq 1$ MHz. This can be explained by the classical concept, where the linewidth of the optical mode a_k can be broadened as $\kappa_{\text{eff}} = \kappa_k + 4|G_{b,k}|^2/\gamma_b$ for the coupling $G_{b,k}a_j^\dagger b_{j-k} + \text{H.c.}$, and the final thermal occupation in equilibrium is calculated by the rate equation as

$$n_f = \frac{\gamma_m n_m}{\gamma_m + \frac{4G_{m,j}^2}{\kappa_{\text{eff}}}}. \quad (26)$$

However, the cooling is greatly enhanced for the strong coupling area with $G_{m,j}/(2\pi) \geq 10$ MHz comparing with no dissipation engineering, and the classical concept no longer holds. For a very strong dissipation engineering coupling strength $G_{b,k}/(2\pi) = 40$ MHz, the red line shows that the cooling effect becomes bad again, and it is due to the frequency shift of the modes for strong dissipation engineering. The modes will become the supermodes, which mean $a_j \Rightarrow (A+B)/\sqrt{2}$ and $b \Rightarrow (B-A)/\sqrt{2}$, and the corresponding frequencies are transformed as $\omega_A = \omega_m - |G_{b,k}|$ and $\omega_B = \omega_m + |G_{b,k}|$. It is obvious that the effective term $G_{m,j}a_j^\dagger m^\dagger + \text{H.c.}$ can not be absolutely eliminated by the rotating wave approximation for strong dissipation engineering. Therefore we can obtain the optimal optomechanical cooling with the increasing of dissipation engineering coupling strength.

For the weak coupling, the dissipation engineering still has a bad effect on the cooling, which is observed by the black dashed line in Fig. 5(b). The blue and red lines show that there is a minimal value of n_f by the dissipation engineering for the strong coupling. Taking the coupling $G_{m,j}$ and the dissipation engineering $G_{b,k}$ into consideration, we plot the Fig. 5(c). It is obviously shown that it can improve the cooling effect by an order of magnitude compared to the case without dissipation engineering.

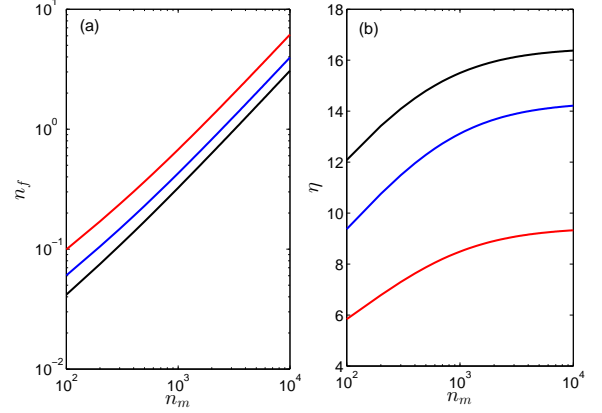


FIG. 6. (Color online) Thermal occupation n_f (a) and the ratio (b) as a function of n_m for $\omega_m/(2\pi) = 50$ (red line), 100 (blue line) and 200 (black line) MHz. Other parameters are the same as Fig. 2.

For different n_m and ω_m , we can always obtain the optimal cooling by tuning the coupling $G_{m,j}$ and the dissipation engineering coupling strength $G_{b,k}$, as shown in Fig. 5(c). In Fig. 6, we discuss the optimal cooling as a function of n_m for $\omega_m/(2\pi) = 50$ (red line), 100 (blue line) and 200 (black line) MHz. From Fig. 6(a), it is observed that the thermal occupation n_f is linear to the thermal noise n_m and the cooling effect is better for the higher frequency ω_m , which is due to the reasonable condition for the rotating wave approximation. Compared with no dissipation engineering $G_{b,k} = 0$, the ratio $\eta = n_{f(G_{b,k}=0)}/n_f$ is plotted in Fig. 6(b), and we observe that the cooling effect is more obvious for the more thermal noise and the ratio value eventually stabilizes. For the frequency ω_m , the ratio has a similar phenomenon with the thermal occupation n_f . In conclusion, we can improve the cooling effect via dissipation engineering by about an order of magnitude for the low-frequency mechanical modes.

V. CONCLUSION

We theoretically studied a multimode optomechanical system and proposed the optomechanical dissipation engineering by an ancilla mechanical mode. It is demonstrated that the dissipation engineering could enhance the system performances on the optomechanical induced transparency and amplification, optomechanical entanglement generation, and the

cooling of the mechanical mode. It is shown that the optomechanical induced transparency and amplification can be enhanced or suppressed due to the controlling of the optical linewidth through coupling to ancilla mechanical mode. In the weak regime of the optomechanical coupling, the thermal noise from the mechanical mode destroys the entanglement between the optical mode and mechanical mode. However, we can recover the entanglement by the anti-Stokes process. In the strong coupling regime, we also find that the optomechanical cooling can be greatly enhanced by dissipation engineering. For the entanglement and cooling, the destruction is from the thermal noise, and the anti-Stokes process provides a cooling effect, which is beneficial to the optomechanical system. However, the strong dissipation engineering ultimately has a bad effect on the multimode optomechanical system because of strong nonlinearity, therefore we can always find the optimal dissipation engineering to realize the best entanglement and cooling. The proposed optomechanical dissipation engineering opens up novel prospects for the phonon-based quantum information processing and macroscopic quantum phenomena.

Acknowledgments. This work was funded by the Key R&D Program of China (Grant No. 2016YFA0301303), the National Natural Science Foundation of China (Grant No.11874342, 11934012, 11922411, 11722436, 11674305 and 11704370), the China Postdoctoral Science Foundation (No. 2019M652181), and Anhui Initiative in Quantum Information Technologies (AHY130200).

* clzou321@ustc.edu.cn

† xbz@ustc.edu.cn

- [1] M. Aspelmeyer, P. Meystre, and K. Schwab, “Quantum optomechanics,” *Physics Today* **65**, 29 (2012).
- [2] T. J. Kippenberg and K. J. Vahala, “Cavity optomechanics: back-action at the mesoscale,” *science* **321**, 1172 (2008).
- [3] D. Van Thourhout and J. Roels, “Optomechanical device actuation through the optical gradient force,” *Nature Photonics* **4**, 211 (2010).
- [4] M. Aspelmeyer, T. J. Kippenberg, and F. Marquardt, “Cavity optomechanics,” *Reviews of Modern Physics* **86**, 1391 (2014).
- [5] S. Weis, R. Rivière, S. Deléglise, E. Gavartin, O. Arcizet, A. Schliesser, and T. J. Kippenberg, “Optomechanically induced transparency,” *Science* **330**, 1520 (2010).
- [6] A. H. Safavi-Naeini, T. M. Alegre, J. Chan, M. Eichenfield, M. Winger, Q. Lin, J. T. Hill, D. E. Chang, and O. Painter, “Electromagnetically induced transparency and slow light with optomechanics,” *Nature* **472**, 69 (2011).
- [7] A. Butsch, J. Koehler, R. Noskov, and P. S. J. Russell, “Cw-pumped single-pass frequency comb generation by resonant optomechanical nonlinearity in dual-nanoweb fiber,” *Optica* **1**, 158 (2014).
- [8] P. B. Deotare, I. Bulu, I. W. Frank, Q. Quan, Y. Zhang, R. Ilıc, and M. Loncar, “All optical reconfiguration of optomechanical filters,” *Nature Communications* **3**, 846 (2012).
- [9] K. Stannigel, P. Komar, S. Habraken, S. Bennett, M. D. Lukin, P. Zoller, and P. Rabl, “Optomechanical quantum information processing with photons and phonons,” *Physical review letters* **109**, 013603 (2012).
- [10] M. R. Vanner, I. Pikovski, G. D. Cole, M. Kim, Č. Brukner, K. Hammerer, G. J. Milburn, and M. Aspelmeyer, “Pulsed quantum optomechanics,” *Proceedings of the National Academy of Sciences* **108**, 16182 (2011).
- [11] G. Anetsberger, E. Gavartin, O. Arcizet, Q. P. Unterreithmeier, E. M. Weig, M. L. Gorodetsky, J. P. Kotthaus, and T. J. Kippenberg, “Measuring nanomechanical motion with an imprecision below the standard quantum limit,” *Physical Review A* **82**, 061804 (2010).
- [12] J. D. Teufel, T. Donner, D. Li, J. W. Harlow, M. Allman, K. Cicak, A. J. Sirois, J. D. Whittaker, K. W. Lehnert, and R. W. Simmonds, “Sideband cooling of micromechanical motion to the quantum ground state,” *Nature* **475**, 359 (2011).
- [13] S. M. Meenehan, J. D. Cohen, G. S. MacCabe, F. Marsili, M. D. Shaw, and O. Painter, “Pulsed excitation dynamics of an optomechanical crystal resonator near its quantum ground state of motion,” *Physical Review X* **5**, 041002 (2015).
- [14] D. Vitali, S. Gigan, A. Ferreira, H. Böhm, P. Tombesi, A. Guerreiro, V. Vedral, A. Zeilinger, and M. Aspelmeyer, “Optomechanical entanglement between a movable mirror and a cavity field,” *Physical review letters* **98**, 030405 (2007).
- [15] X. Yang, Z. Yin, and M. Xiao, “Optomechanically induced entanglement,” *Physical Review A* **99**, 013811 (2019).
- [16] X.-Y. Lü, J.-Q. Liao, L. Tian, and F. Nori, “Steady-state mechanical squeezing in an optomechanical system via duffing nonlinearity,” *Physical Review A* **91**, 013834 (2015).
- [17] D. Branford, H. Miao, and A. Datta, “Fundamental quantum limits of multicarrier optomechanical sensors,” *Physical review letters* **121**, 110505 (2018).
- [18] O. Arcizet, P.-F. Cohadon, T. Briant, M. Pinard, A. Heidmann, J.-M. Mackowski, C. Michel, L. Pinard, O. Français, and L. Rousseau, “High-sensitivity optical monitoring of a micromechanical resonator with a quantum-limited optomechanical sensor,” *Physical review letters* **97**, 133601 (2006).
- [19] D. Lee, M. Underwood, D. Mason, A. Shkarin, S. Hoch, and J. Harris, “Multimode optomechanical dynamics in a cavity with avoided crossings,” *Nature communications* **6**, 6232 (2015).
- [20] L. Fan, K. Y. Fong, M. Poot, and H. X. Tang, “Cascaded optical transparency in multimode-cavity optomechanical systems,” *Nature communications* **6**, 5850 (2015).
- [21] R. Duggan, J. del Pino, E. Verhagen, and A. Alù, “Optomechanically induced birefringence and optomechanically induced faraday effect,” *Physical Review Letters* **123**, 023602 (2019).
- [22] X. Wei, J. Sheng, C. Yang, Y. Wu, and H. Wu, “Controllable two-membrane-in-the-middle cavity optomechanical system,” *Physical Review A* **99**, 023851 (2019).
- [23] Z. Shen, Y.-L. Zhang, Y. Chen, C.-L. Zou, Y.-F. Xiao, X.-B. Zou, F.-W. Sun, G.-C. Guo, and C.-H. Dong, “Experimental realization of optomechanically induced non-reciprocity,” *Nature Photonics* **10**, 657 (2016).
- [24] F. Ruesink, J. P. Mathew, M.-A. Miri, A. Alù, and E. Verhagen, “Optical circulation in a multimode optomechanical resonator,” *Nature communications* **9**, 1798 (2018).
- [25] Z. Shen, Y.-L. Zhang, Y. Chen, F.-W. Sun, X.-B. Zou, G.-C. Guo, C.-L. Zou, and C.-H. Dong, “Reconfigurable optomechanical circulator and directional amplifier,” *Nature communications* **9**, 1797 (2018).
- [26] C. Dong, V. Fiore, M. C. Kuzyk, and H. Wang, “Optomechanical dark mode,” *Science* **338**, 1609 (2012).

- [27] J. T. Hill, A. H. Safavi-Naeini, J. Chan, and O. Painter, “Coherent optical wavelength conversion via cavity optomechanics,” *Nature communications* **3**, 1196 (2012).
- [28] F. Verstraete, M. M. Wolf, and J. I. Cirac, “Quantum computation and quantum-state engineering driven by dissipation,” *Nature physics* **5**, 633 (2009).
- [29] J. Poyatos, J. I. Cirac, and P. Zoller, “Quantum reservoir engineering with laser cooled trapped ions,” *Physical review letters* **77**, 4728 (1996).
- [30] K. Stannigel, P. Rabl, and P. Zoller, “Driven-dissipative preparation of entangled states in cascaded quantum-optical networks,” *New Journal of Physics* **14**, 063014 (2012).
- [31] A. Sarlette, J.-M. Raimond, M. Brune, and P. Rouchon, “Stabilization of nonclassical states of the radiation field in a cavity by reservoir engineering,” *Physical review letters* **107**, 010402 (2011).
- [32] Z. Leghtas, U. Vool, S. Shankar, M. Hatridge, S. M. Girvin, M. H. Devoret, and M. Mirrahimi, “Stabilizing a bell state of two superconducting qubits by dissipation engineering,” *Physical Review A* **88**, 023849 (2013).
- [33] S.-l. Ma, X.-k. Li, X.-y. Liu, J.-k. Xie, and F.-l. Li, “Stabilizing bell states of two separated superconducting qubits via quantum reservoir engineering,” *Physical Review A* **99**, 042336 (2019).
- [34] J. T. Barreiro, M. Müller, P. Schindler, D. Nigg, T. Monz, M. Chwalla, M. Hennrich, C. F. Roos, P. Zoller, and R. Blatt, “An open-system quantum simulator with trapped ions,” *Nature* **470**, 486 (2011).
- [35] P. Schindler, M. Müller, D. Nigg, J. T. Barreiro, E. A. Martinez, M. Hennrich, T. Monz, S. Diehl, P. Zoller, and R. Blatt, “Quantum simulation of dynamical maps with trapped ions,” *Nature Physics* **9**, 361 (2013).
- [36] P.-B. Li, S.-Y. Gao, and F.-L. Li, “Engineering two-mode entangled states between two superconducting resonators by dissipation,” *Physical Review A* **86**, 012318 (2012).
- [37] D.-X. Li, X.-Q. Shao, J.-H. Wu, X. Yi, and T.-Y. Zheng, “Engineering steady knill-lafamme-milburn state of rydberg atoms by dissipation,” *Optics express* **26**, 2292 (2018).
- [38] F. Massel, S. U. Cho, J.-M. Pirkkalainen, P. J. Hakonen, T. T. Heikkilä, and M. A. Sillanpää, “Multimode circuit optomechanics near the quantum limit,” *Nature communications* **3**, 987 (2012).
- [39] Z. J. Deng, X.-B. Yan, Y.-D. Wang, and C.-W. Wu, “Optimizing the output-photon entanglement in multimode optomechanical systems,” *Physical Review A* **93**, 033842 (2016).
- [40] C. Ockeloen-Korppi, M. Gely, E. Damskägg, M. Jenkins, G. Steele, and M. Sillanpää, “Sideband cooling of nearly degenerate micromechanical oscillators in a multimode optomechanical system,” *Physical Review A* **99**, 023826 (2019).
- [41] Y.-L. Zhang, C.-H. Dong, C.-L. Zou, X.-B. Zou, Y.-D. Wang, and G.-C. Guo, “Optomechanical devices based on traveling-wave microresonators,” *Physical Review A* **95**, 043815 (2017).
- [42] W. H. P. Nielsen, Y. Tsaturyan, C. B. Møller, E. S. Polzik, and A. Schliesser, “Multimode optomechanical system in the quantum regime,” *Proceedings of the National Academy of Sciences* **114**, 62 (2017).
- [43] P. Meystre, “A short walk through quantum optomechanics,” *Annalen der Physik* **525**, 215 (2013).
- [44] J. H. Lee and H. Seok, “Quantum reservoir engineering through quadratic optomechanical interaction in the reversed dissipation regime,” *Physical Review A* **97**, 013805 (2018).
- [45] R.-X. Chen, C.-G. Liao, and X.-M. Lin, “Dissipative generation of significant amount of mechanical entanglement in a coupled optomechanical system,” *Scientific Reports* **7**, 14497 (2017).
- [46] X.-X. Hu, C.-L. Zhao, Z.-B. Wang, Y.-L. Zhang, X.-B. Zou, C.-H. Dong, H. X. Tang, G.-C. Guo, and C.-L. Zou, “Cavity-enhanced optical controlling based on three-wave mixing in cavity-atom ensemble system,” *Optics express* **27**, 6660 (2019).
- [47] M. H. Devoret and R. J. Schoelkopf, “Superconducting circuits for quantum information: an outlook,” *Science* **339**, 1169 (2013).
- [48] M. Wallquist, K. Hammerer, P. Rabl, M. Lukin, and P. Zoller, “Hybrid quantum devices and quantum engineering,” *Physica Scripta* **2009**, 014001 (2009).
- [49] Y.-D. Wang and A. A. Clerk, “Reservoir-engineered entanglement in optomechanical systems,” *Physical review letters* **110**, 253601 (2013).
- [50] L. Tian, “Robust photon entanglement via quantum interference in optomechanical interfaces,” *Physical review letters* **110**, 233602 (2013).
- [51] M. J. Hartmann and M. B. Plenio, “Steady state entanglement in the mechanical vibrations of two dielectric membranes,” *Physical Review Letters* **101**, 200503 (2008).
- [52] X. Zhang, N. Zhu, C.-L. Zou, and H. X. Tang, “Optomagnonic whispering gallery microresonators,” *Physical review letters* **117**, 123605 (2016).
- [53] L. Pezzè, A. Smerzi, M. K. Oberthaler, R. Schmied, and P. Treutlein, “Quantum metrology with nonclassical states of atomic ensembles,” *Reviews of Modern Physics* **90**, 035005 (2018).
- [54] E. Viasnoff-Schwoob, C. Weisbuch, H. Benisty, C. Cuisin, E. Derouin, O. Drisse, G. H. Duan, L. Legouezigou, O. Legouezigou, F. Pommereau, *et al.*, “Compact wavelength monitoring by lateral outcoupling in wedged photonic crystal multimode waveguides,” *Applied Physics Letters* **86**, 101107 (2005).
- [55] C.-H. Dong, Z. Shen, C.-L. Zou, Y.-L. Zhang, W. Fu, and G.-C. Guo, “Brillouin-scattering-induced transparency and non-reciprocal light storage,” *Nature communications* **6**, 6193 (2015).
- [56] I. S. Grudinin, H. Lee, O. Painter, and K. J. Vahala, “Phonon laser action in a tunable two-level system,” *Physical review letters* **104**, 083901 (2010).
- [57] C. Weedbrook, S. Pirandola, R. García-Patrón, N. J. Cerf, T. C. Ralph, J. H. Shapiro, and S. Lloyd, “Gaussian quantum information,” *Reviews of Modern Physics* **84**, 621 (2012).
- [58] M. B. Plenio, “Logarithmic negativity: a full entanglement monotone that is not convex,” *Physical review letters* **95**, 090503 (2005).
- [59] E. X. DeJesus and C. Kaufman, “Routh-hurwitz criterion in the examination of eigenvalues of a system of nonlinear ordinary differential equations,” *Physical Review A* **35**, 5288 (1987).